

Molecular dynamics simulation of RGD peptide adsorption on titanium oxide surfaces

Hong-Ping Zhang · Xiong Lu · Li-Ming Fang ·
Jie Weng · Nan Huang · Yang Leng

Received: 4 December 2007 / Accepted: 6 June 2008 / Published online: 27 June 2008
© Springer Science+Business Media, LLC 2008

Abstract Peptide Arg–Gly–Asp (RGD) sequence is a ubiquitous adhesive motif found in various bone extracellular matrix proteins and is crucial in the biomaterial surface/interface reaction. This study analyzed the adsorption of RGD on different titanium oxide surfaces with molecular dynamics simulation. The simulation results indicate that the RGD peptide binds strongly with anatase (001) and rutile (010). RGD conformation changes due to the variation of the backbone torsion angle in the middle of the RGD chain. Pair correlation function analysis indicates that the interaction of the RGD peptide and the titanium oxide results from hydrogen bonding and the groups in RGD play different roles during the adsorption process. This study provides useful information on how to design titanium surfaces in order to modulate peptide or protein adsorption.

1 Introduction

Titanium and its alloys have been widely used as materials for medical implants in human body since late 1970s [1].

H.-P. Zhang · X. Lu (✉) · J. Weng · N. Huang
Key Lab of Advanced Technologies of Materials, Ministry of Education, School of Materials Science and Engineering, Southwest Jiaotong University, Chengdu, Sichuan 610031, China
e-mail: luxiong_2004@163.com

L.-M. Fang
Department of Polymer Science and Engineering, School of Materials Science and Engineering, South China University of Technology, Guangzhou, Guangdong 510641, China

L.-M. Fang · Y. Leng
Department of Mechanical Engineering, Hong Kong University of Science and Technology, Kowloon, Hong Kong, China

The thin layer of native titanium oxide on titanium surface, formed by reacting with biological fluids, was believed to be closely related to titanium excellent biocompatibility and osteointegration [2]. There are three types of TiO_2 , i.e., rutile, anatase, and brookite. The crystal surfaces of rutile (110), (100), (001), (010) and anatase (101), (100), (001), (010) are of most interest in the surface science of TiO_2 [3].

Peptide-based biomaterials are usually adsorbed on TiO_2 surfaces to give rise to self-organized two- and three-dimensional structures, which support three-dimensional tissue growth. Therefore, various peptides and proteins have been grafted on TiO_2 surfaces by different methods to enhance bone growth on implant surfaces [4]. Peptide Arg–Gly–Asp (RGD) sequence is a ubiquitous adhesive motif that is found in various bone extracellular matrix proteins such as collagen, fibronectin, osteonectin, and vitronectin [5]. Since RGD peptide has profound effects on the osteoblast adhesion, it has been suggested to graft RGD on titanium surfaces in order to increase the osteoblast adhesion to and subsequent proliferation on orthopedic implants [6, 7].

Understanding the adsorption and interaction of RGD peptide on TiO_2 surfaces is crucial for successfully grafting RGD on the surfaces of titanium implants. Few theoretical studies have been reported in this aspect although the interaction between the RGD peptide and TiO_2 has been investigated by experiments both in vitro and in vivo [8–10]. Molecular dynamics (MD) simulation is able to reveal the microscopic interactions at the atomic scale and can help in comprehensive understanding and interpreting the experiment results [11]. In this study, MD simulations were performed to investigate the interfacial behavior between the RGD peptide and various TiO_2 surfaces. The binding energies, torsion angles, and pair correlation functions (PCF) during the process of RGD

adsorption on TiO_2 surfaces were analyzed in order to understand the interaction mechanism.

2 Methods and model

The MD simulations were conducted with the Materials Studio v.4.1 packages (Accelrys, San Diego, CA) using the force field of the condensed-phase optimized molecular potentials for atomistic simulation studies (COMPASS), which is a “Class II” ab initio-based force field and is applicable to both organic and inorganic materials [12–14]. Using COMPASS resulted in a compromise between the accuracy and availability of force field parameters for all atom types presenting in the current simulation model [15]. Canonical (NVT) ensemble was used in the MD simulations where the Nosé algorithm method was used for the temperature control.

2.1 RGD peptide

The peptide chain was constructed by adding the amino acid residues with the sequence of Arg–Gly–Asp (Fig. 1). Figure 1a schematically showed the torsion angles that were monitored through MD simulation. Figure 1a also indicates the interesting atoms in the pair correction function (PCF) analysis. To obtain the RGD conformation that exhibits minimized energy, the chain was annealed by MD simulations for 100 ps at each temperature with the temperature increasing from 298 K in steps of 10 K to 338 K and decreasing back.

2.2 TiO_2 surfaces

TiO_2 surfaces were constructed by cleaving the crystal along certain crystallographic planes, namely, (110), (100), (001), and (010) for rutile, while (101), (100), (001), and (010) for anatase. The dimensions of the rutile surfaces in the simulation were as follows: (001) 44 Å × 37 Å × 11 Å; (010) 38 Å × 36 Å × 11 Å; (100) 46 Å × 46 Å × 11 Å; (110) 35 Å × 39 Å × 11 Å. The dimensions of the anatase surfaces in the simulation were as follows: (001) 38 Å × 38 Å × 11 Å; (010) 38 Å × 38 Å × 11 Å; (100) 38 Å × 38 Å × 11 Å; (110) 41 Å × 38 Å × 11 Å. The first two layers of each surface was annealed in the temperature range of 300–500 K with the step size of 20 K at each temperature for 100 ps by MD simulations. The annealing generated atomistic disorders on TiO_2 surfaces, similar to the real surfaces.

2.3 RGD– TiO_2 system

RGD peptide with the minimum energy conformation was placed close to each TiO_2 surface with random orientation.

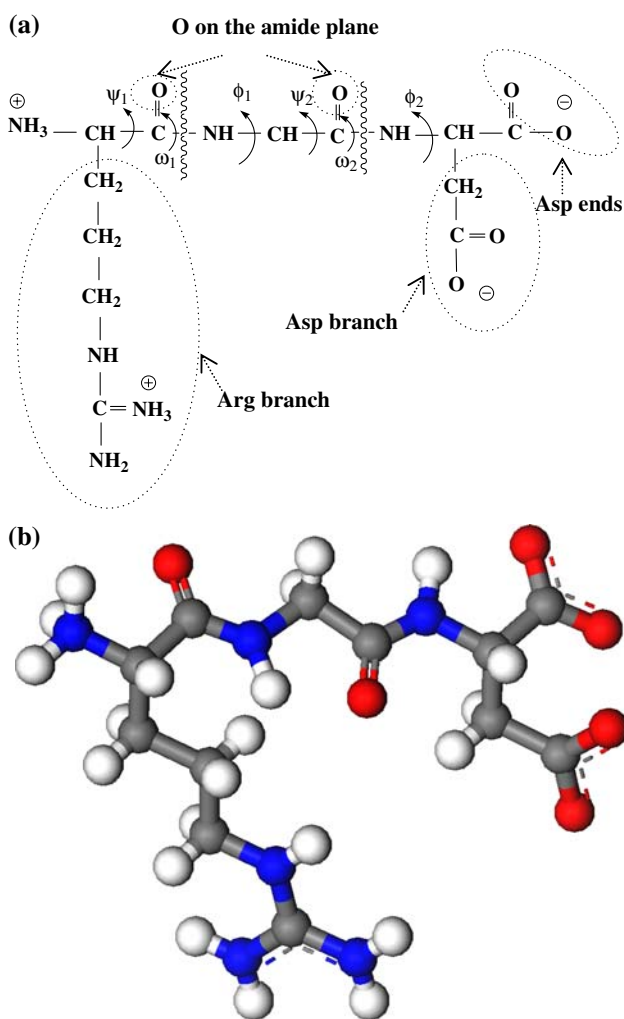


Fig. 1 (a) Schematic drawing of RGD peptide structure, including the index of the interested torsion angles and atom groups; (b) Ball-and-Stick model of RGD and the color codes: carbon, gray; hydrogen, white; nitrogen, blue; and oxygen, red

A vacuum slab with the thickness of 30 Å was added above the TiO_2 surfaces so that a RGD chain only interacted with one side of the surfaces (Fig. 2). Finally, the conformation of the RGD– TiO_2 system was analyzed by minimizing the total energy through MD simulations and the MD trajectory was stored for subsequent analysis.

3 Results and discussion

3.1 Binding energy

The binding energy between the RGD peptide and the TiO_2 surface can be calculated using the following formula:

$$E_{\text{binding}} = (E_{\text{TiO}_2} + E_{\text{RGD}}) - E_{\text{total}}$$

in which E_{total} is the total energy of the RGD– TiO_2 system; E_{TiO_2} is the energy of the TiO_2 surface without the RGD, and

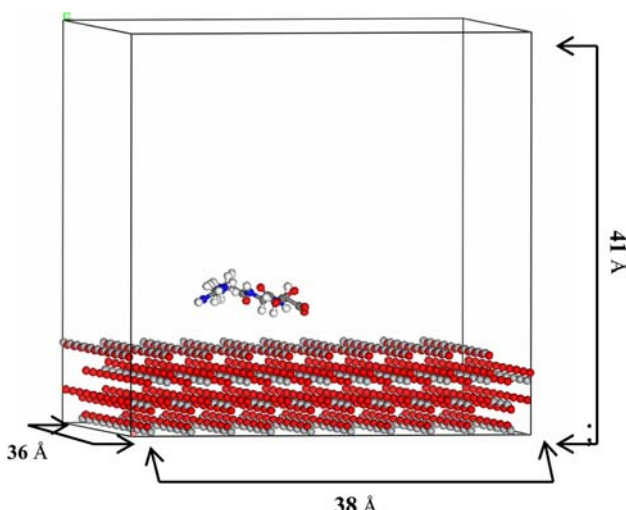


Fig. 2 RGD–TiO₂ interaction model used for MD simulation

E_{RGD} is the energy of the RGD without the TiO₂ surface [16, 17]. Table 1 lists all the binding energies per unit surface area obtained from MD simulations. For anatase, RGD adsorption on the (001) surface has the highest binding energy, indicating the strongest interaction. The binding energies of RGD peptide on (010) and (100) surfaces are at the same level and both are much lower than those of (001) and (101). For rutile, the RGD peptide shows the highest binding energy on the (010) surface than on other three surfaces. Figure 3 shows snapshots of the RGD peptide configurations on the various surfaces. The simulations indicate that the RGD peptide manifests a similar conformation on both anatase (001) and rutile (010). This simulation results imply that this RGD peptide conformation is related to a tight binding form of RGD on titanium surfaces.

3.2 Torsion angle

Analysis of torsion angle variations of molecules help us to understand the conformational changes of RGD peptide

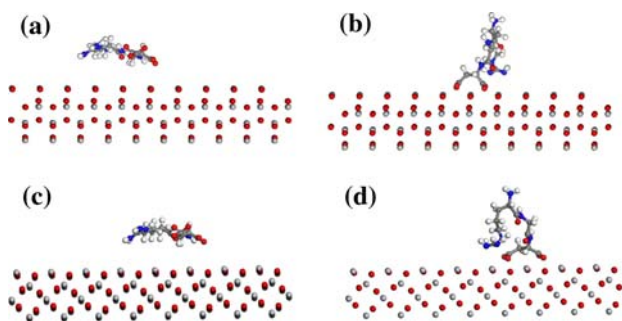


Fig. 3 The snapshot of the RGD peptide configuration: RGD peptide on the anatase (001) surface before (a) and after (b) MD simulation; RGD peptide on the rutile surface (010) before (c) and after (d) MD simulation

during the adsorption process [18]. The torsion angle variations during RGD adsorption on the surfaces were monitored; particularly, for the adsorption with the highest binding energy, rutile (010) and anatase (001). The ω_1 and ω_2 torsion angles locating on the amide plane keep constant during the whole MD process. This result indicates that the simulation is reasonable because the ω_1 and ω_2 should be $\pm 180^\circ$ according to the general theory of biochemistry. Figure 4 shows that the RGD peptide backbone torsion angles (ϕ_1 and ψ_2) change drastically at the beginning of the adsorption process, approximately within 3 ps, when RGD interacts with anatase (001). The torsion angle ϕ_1 keeps a nearly constant value of -100° after an acute change at approximately 2 ps while ψ_1 keeps the constant of 100° . However, the torsion angle ψ_2 fluctuates in the range of -180° to 0° and finally falls in the range of -150° to -100° , while ϕ_2 maintains at -100° after the initial vibration stage. The torsion angles of RGD peptide adsorbing on the rutile (010) shows the similar change patterns (Fig. 5). In summary, torsion angle analysis indicates that the conformation change during RGD adsorption on titanium oxide surface is mainly caused by the changes of ψ_2 , the back bone torsion angle in the middle of the RGD chain.

Table 1 The binding energy between the RGD peptide and the TiO₂ surfaces of two crystal forms

TiO ₂ Surfaces	Surface area (Å ²)	E_{total} (kcal/mol)	E_{TiO_2} (kcal/mol)	E_{RGD} (kcal/mol)	E_{binding} (kcal/mol)	$E_{\text{binding-unit area}}$ (kcal/mol Å ²)
A (001)	1426	-750362	-750362	-48	1596	1.13
A (010)	1433	-769043	-768689	-280	74	0.05
A (100)	1433	-769165	-768810	-300	55	0.04
A (101)	1542	-789361	-788029	-47	1285	0.83
R (001)	1631	-1611316	-1609921	-21	1374	0.84
R (010)	1414	-839803	-838079	-35	1689	1.19
R (100)	2110	-1149326	-1148994	-281	51	0.02
R (110)	1384	-924958	-923758	-81	1119	0.81

A, anatase; R, rutile

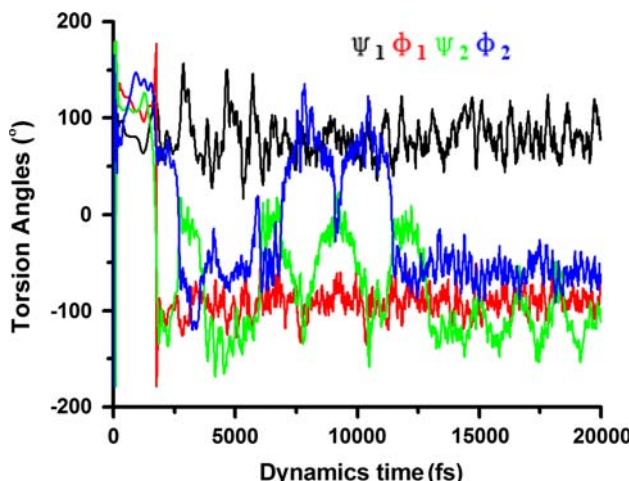


Fig. 4 The torsion angle (ψ_1 , ϕ_1 , ψ_2 and ϕ_2) evolution with time of RGD peptide on the anatase (001) during the MD simulation process

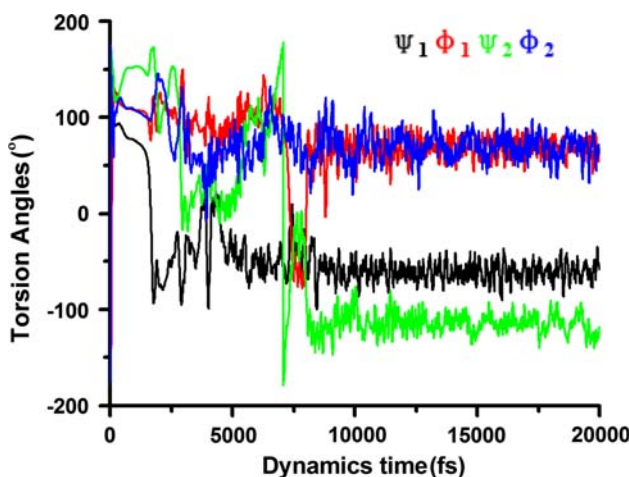


Fig. 5 The torsion angle (ψ_1 , ϕ_1 , ψ_2 and ϕ_2) evolution with time of RGD peptide on the rutile (010) during the MD simulation process

3.3 Pair correlation function

The PCF analysis indicates that the behavior of RGD adsorption on different surfaces is quite similar, and the interaction between the RGD peptide and the titanium oxide surface mainly results from hydrogen bonding. As indicated in Fig. 6, the main contribution of the interaction comes from the strong interaction between the Ti atoms of the very top titanium oxide surface and the O atoms locating at the end or at the branch of the Asp residues because the first strong peak is at the round of 2.5 Å, which is a typical hydrogen bonding [19, 20]. The PCF analysis also indicates that different groups in RGD play different roles during the RGD adsorption process. Figure 6 shows that the peak of Ti–O(Asp end) in RGD–rutile is larger than that in RGD–anatase while the peak of Ti–Asp branch in RGD–rutile is lower than that in RGD–anatase.

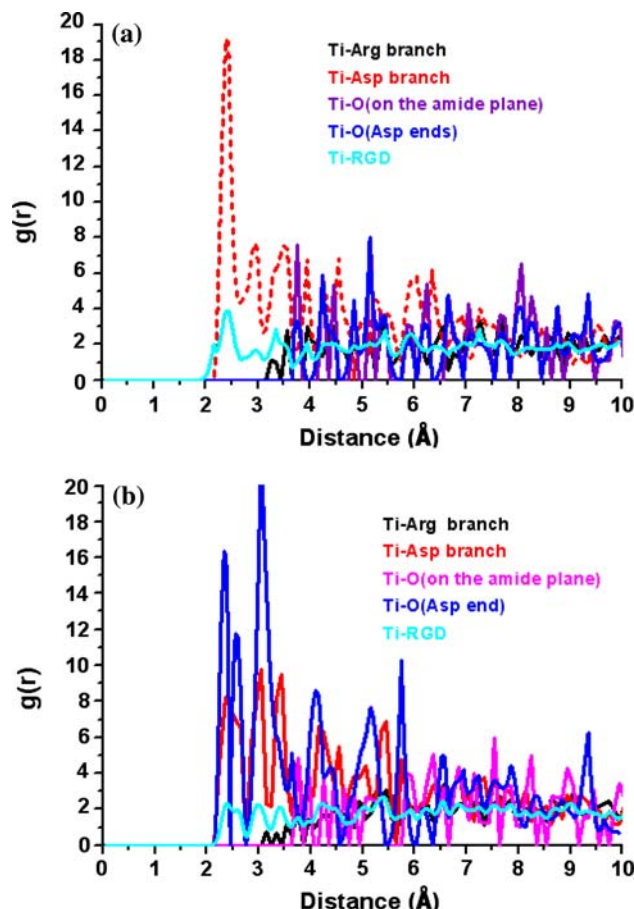


Fig. 6 The pair correlation functions: (a) RGD–anatase (001); and (b) RGD–rutile (010)

However, there is not much PCF difference in the interactions of Ti–Arg branch and Ti–O (on the amide plane). Their interaction distances are in the range of 3–4 Å for RGD–anatase and RGD–rutile.

4 Conclusions

MD simulations of adsorptions of RGD peptide on titanium oxide surfaces indicate that the RGD peptide has high binding energy on anatase (001) and rutile (010). RGD conformation change is mainly caused by the change of the back bone torsion angle in the middle of the RGD chain. PCF analysis indicates that the RGD peptide and the titanium oxide generate hydrogen bonding and different groups in RGD play various roles during the adsorption process.

Acknowledgments This project was financially supported by the National Natural Science Foundation of China (No. 30700172), Specialized Research Fund for the Doctoral Program of Higher Education for Young Teacher (20070613019) and National Key Project of Scientific and Technical Supporting Programs Fund from MSTD (2006BAI16B01).

References

1. A. Thor, L. Rasmusson, A. Wennerberg, P. Thomsen, J.-M. Hirsch, B. Nilsson et al., *Biomaterials* **28**, 966 (2007). doi:[10.1016/j.biomaterials.2006.10.020](https://doi.org/10.1016/j.biomaterials.2006.10.020)
2. Y. Wang, O. Warschkow, L.D. Marks, *Surf. Sci.* **601**, 63 (2007). doi:[10.1016/j.susc.2006.09.005](https://doi.org/10.1016/j.susc.2006.09.005)
3. U. Diebold, *Surf. Sci. Rep.* **48**, 53 (2003). doi:[10.1016/S0167-5729\(02\)00100-0](https://doi.org/10.1016/S0167-5729(02)00100-0)
4. D.M. Ferris, G.D. Moodie, P.M. Dimond, C.W.D. Giorani, M.G. Ehrlich, R.F. Valentini, *Biomaterials* **20**, 2323 (1999). doi:[10.1016/S0142-9612\(99\)00161-1](https://doi.org/10.1016/S0142-9612(99)00161-1)
5. B. Elmengaard, J.E. Bechtold, K. Soballe, *Biomaterials* **26**, 3521 (2005). doi:[10.1016/j.biomaterials.2004.09.039](https://doi.org/10.1016/j.biomaterials.2004.09.039)
6. M. Schuler, G.R. Owen, D.W. Hamilton, M. de Wild, M. Textor, D.M. Brunette et al., *Biomaterials* **27**, 4003 (2006). doi:[10.1016/j.biomaterials.2006.03.009](https://doi.org/10.1016/j.biomaterials.2006.03.009)
7. S. Tosatti, S.M.D. Paul, A. Askendal, S. VandeVondele, J.A. Hubbell, P. Tengvall et al., *Biomaterials* **24**, 4949 (2003). doi:[10.1016/S0142-9612\(03\)00420-4](https://doi.org/10.1016/S0142-9612(03)00420-4)
8. B. Zhao, W. Tian, H. Feng, I.-S. Lee, F. Cui, *Curr. Appl. Phys.* **5**, 407 (2005). doi:[10.1016/j.cap.2005.01.002](https://doi.org/10.1016/j.cap.2005.01.002)
9. G. Iucci, M. Dettin, C. Battocchio, R. Gambaretto, C.D. Bello, G. Polzonetti, *Mat. Sci. Eng. C* **27**, 1201 (2007)
10. S. Rammelt, T. Illert, S. Bierbaum, D. Scharnweber, H. Zwipp, W. Schneiders, *Biomaterials* **27**, 5561 (2006). doi:[10.1016/j.biomaterials.2006.06.034](https://doi.org/10.1016/j.biomaterials.2006.06.034)
11. H.J.C.B. Wilfred, F. van Gunsteren, *Angew. Chem. Int. Ed. Engl.* **29**, 992 (1990). doi:[10.1002/anie.199009921](https://doi.org/10.1002/anie.199009921)
12. H. Sun, *J. Phys. Chem. B* **102**, 7338 (1998). doi:[10.1021/jp980939v](https://doi.org/10.1021/jp980939v)
13. H. Sun, P. Ren, J.R. Fried, *Comput. Theor. Polym. Sci.* **8**, 229 (1998). doi:[10.1016/S1089-3156\(98\)00042-7](https://doi.org/10.1016/S1089-3156(98)00042-7)
14. H. Sun, P.W.C. Kung, *J. Comput. Chem.* **26**, 169 (2005). doi:[10.1002/jcc.20153](https://doi.org/10.1002/jcc.20153)
15. R. Toth, M. Ferrone, S. Miertus, E. Chiellini, M. Fermeglia, S. Pricl, *Biomacromolecules* **7**, 1714 (2006). doi:[10.1021/bm050937y](https://doi.org/10.1021/bm050937y)
16. R. Bhowmik, K.S. Katti, D. Katti, *Polymer (Guildf)* **48**, 664 (2007). doi:[10.1016/j.polymer.2006.11.015](https://doi.org/10.1016/j.polymer.2006.11.015)
17. T.R. Rybolt, C.E. Wells, C.R. Sisson, C.B. Black, K.A. Ziegler, J. Colloid. Interf. Sci. **314**, 434 (2007). doi:[10.1016/j.jcis.2007.05.083](https://doi.org/10.1016/j.jcis.2007.05.083)
18. S. Monti, V. Caravetta, W. Zhang, J. Yang, *J. Phys. Chem. C* **111**, 7765 (2007). doi:[10.1021/jp071095v](https://doi.org/10.1021/jp071095v)
19. N. Kantarci, C. Tamerler, M. Sarikaya, T. Haliloglu, P. Doruker, *Polymer (Guildf)* **46**, 4307 (2005)
20. Z. Yang, Y.-P. Zhao, *Eng. Anal. Bound. Elem.* **31**, 402 (2007). doi:[10.1016/j.enganabound.2006.07.012](https://doi.org/10.1016/j.enganabound.2006.07.012)